

## CHAPTER 73

### DAMAGE ANALYSIS FOR RUBBLE-MOUND BREAKWATERS

Michael H. Davies  
Etienne P.D. Mansard, and  
Andrew M. Cornett<sup>1</sup>

#### Abstract

Storm damage to rubble-mound structures can range from the piece-wise removal of individual armour stones to the large-scale sliding of the entire armour layer. This paper presents an overview of qualitative and quantitative descriptions of various types of armour layer damage due to wave action. This work is based on a series of large-scale physical models of revetment stability. The discussion includes methods for measuring the change in profile and the use of the normalized area eroded,  $S$ . A new parameter,  $d_c$  is introduced as a measure of the minimum depth of cover remaining on the structure. An analysis method is presented which predicts the armour layer's factor of safety against sliding.

#### Introduction

Coastal structures are often designed to survive severe storms with no significant damage while undergoing tolerable damage during more extreme events. For such designs it is essential that the damage be both predictable and repairable - the failure mode should be ductile not brittle. Physical hydraulic models are a key tool in the design of structures where damage levels need to be determined. In addition to accurately reproducing the wave loading on the structure and the physical characteristics of the structure it is important to be able to accurately measure and quantify the damage which occurs.

#### Damage analysis

The two common measures for rubble-mound damage due to wave action are visual assessment and profiling. Visual assessment includes the monitoring of the development of holes in the armour, observation of the exposure of under-layers and counting the number of armour units displaced. Profile analysis includes measurement of the eroded profile and calculation of the eroded cross-sectional area,  $A$ .

---

<sup>1</sup> Coastal Engg. M-32, Institute for Marine Dynamics, National Research Council Canada, Montreal Rd, Ottawa, Ontario, K1A 0R6.

At low damage levels the breakwater damage can be readily estimated by visually counting the number of rocks displaced. This becomes difficult however, when more than, say, 50 stones are displaced or when stones which have been moved slightly by one storm condition are subsequently moved further downslope by a subsequent storm sequence. Image processing allows visual techniques to be used at higher damage levels. The size of the damaged area can be measured using photogrammetry and digital image processing. Also, the movement of individual stones can be tracked using image processing software. The limitations on these techniques are that it is often necessary to drain the basin prior to image-capture to allow measurement below the still water line and that image quality can restrict accuracy. Furthermore, most techniques allow an estimation of only the damaged surface area, not the depth of penetration of the damage. This can sometimes be overcome by colour coding the various layers of revetment.

For damage quantification based on stone count, the 1984 Shore Protection Manual (CERC, 1984) defines damage as the percentage of stones removed from within the active zone. The active zone is defined as extending from the middle of the breakwater crest down to one zero-damage wave height below the still water level.

$$\text{Damage (\%)} = \frac{\text{Number of stones removed}}{\text{Number of stones within active zone}} \times 100 \quad (1)$$

This has the limitation that it depends on visual stone counts (which can be unreliable at higher damage levels) and that the number of stones within the active zone is very dependent upon structure geometry.

Several mechanical and electro-mechanical profiling methods exist for the determination of breakwater profile. All have their limitations. The more sophisticated profilers which operate on the principles of electrical resistivity or light or acoustic beams to locate the profile generally require the flume to be either fully drained or fully flooded so that measurements are made in either the dry or in the wet - measurement through the air-water interface is difficult. The need to flood or drain the basin between each test sequence can be very time consuming. Measurement methods which use mechanical contact with the rocks to locate the profile can readily cross the air-water interface but often provide lower resolution and sparser data.

Measurement of the cross-sectional profile is often the fastest and most reliable means of damage assessment and is used in most hydraulics laboratories. Hughes (1993) reviews some of the visual and profiling methods available for damage analysis. Van der Meer (1988) reports on the use of a mechanical profiler for measuring damage to rubble-mound breakwaters. Latham et al. (1988) report on the use of high resolution mechanical profiling methods for breakwater damage analysis. Medina et al. (1994) reports on the use of mechanical profiles for damage analysis.

If profiles of the damaged cross-section are obtained, the damage can be represented by the mean cross-sectional area removed from the profile,  $A$ . In this analysis the eroded quantity,  $A$  is determined by integration of the difference between the damaged and initial profiles. The most widely accepted method for interpreting the damage data from profiling is the damage index,  $S$  as adopted by van der Meer. The damage index,

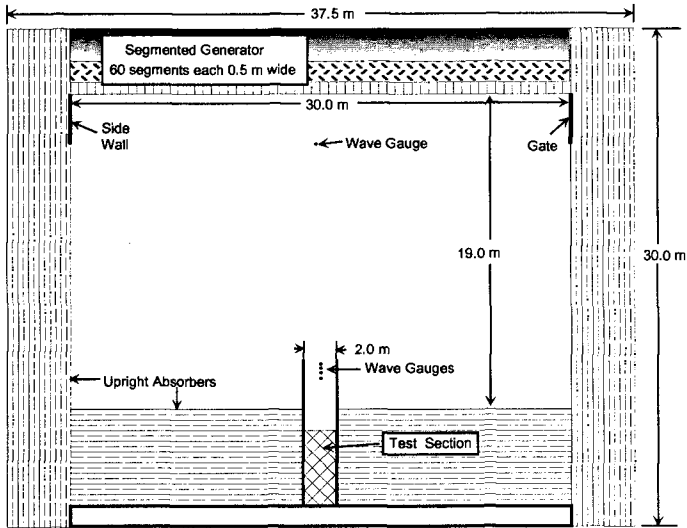


Figure 1 Test configuration for NRC revetment stability study.

S is defined as:

$$S = \frac{A}{D_{n50}^2} \quad \text{where } D_{n50} = \sqrt[3]{\frac{M_{50}}{\rho_s}} \quad (2)$$

S corresponds to the number of cubic stones of size  $D_{n50}$  removed from the average profile line.  $M_{50}$  is the median of the cumulative stone mass distribution and  $\rho_s$  is the density of stone (typically  $2,650 \text{ kg/m}^3$ ).

For comparison between counted stone damage and profile analysis a visual estimate of the damage,  $S_{\text{visual}}$  can be derived as follows:

$$S_{\text{visual}} = \frac{\# \text{ stones removed}}{(\text{Structure width}/D_{n50})(1-n)} \quad (3)$$

Here n is the placement density determined by profiling the armour and underlayers and from knowing the total mass of rock placed.

**NRC Experiments on breakwater damage**

NRC has recently completed a series of large-scale 2-D experiments on revetment stability for the Société d'énergie de la Baie James. This study examined the existing revetment along with proposed repair schemes for some of the earth dams and dykes of the La Grande hydroelectric complex near James Bay in northern Québec. Some details of this model study are reviewed in Mansard et al (1994). This test series was performed in the NRC Multi-directional Wave Basin at scales ranging from 1:10 to 1:15

depending on the structure being tested. Figure 1 shows the experimental setup used for these tests. The wave climates used in the tests were calibrated prior to installation of the structures in the test section to allow determination of the time-domain characteristics of the incident wave climate in the absence of reflections from the structure. The results from some of the testing performed in this study will be used in this paper to illustrate various damage analysis methods.

The NRC breakwater profiler (shown schematically in Figure 2) uses a carriage-mounted mechanical pivoting arm to track the breakwater profile. The arm is connected to a rotational potentiometer which measures the angle of declination,  $\theta$ . The horizontal location of the carriage,  $R$  is measured using a potentiometer connected to the cable system which drives the carriage. The contact point between the rotating arm and the armour layer is a wheel of diameter roughly equal to the mean stone size,  $D_{50}$ . Thus each profile is averaged mechanically so that gaps in the armour layer smaller than  $D_{50}$  are ignored. Output from the two potentiometers is sampled at 20Hz using the NRC Gedap data acquisition and analysis system. In processing, the data files,  $R(t)$  and  $\theta(t)$  are reduced to a single file containing  $z(x)$  using the relationships:

$$\begin{aligned} x &= R - L \cos(\theta) \quad \text{and} \\ z &= (\text{Elevation of beam}) - L \sin(\theta) \quad \text{where } L \text{ is the profile rod length.} \end{aligned} \tag{4}$$

Typically nine evenly-spaced profile lines are measured. Analysis can be performed on individual profile lines to obtain details on the spatial distribution of damage or the measured profile lines can first be averaged then integrated. The cross-sectional area of material eroded from the armour layer is determined by integration using Simpson's method,  $A_1(x)$ :

$$A_1(x) = \int_{x_0}^x [z_1(x) - z_0(x)] dx \tag{5}$$

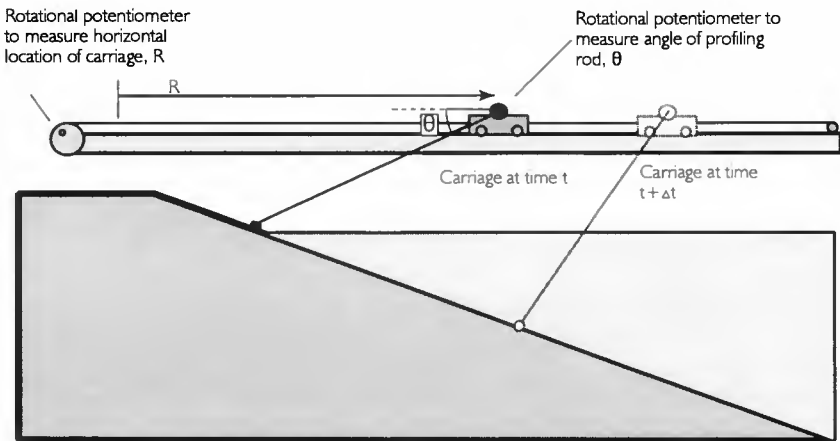


Figure 2 NRC electro-mechanical profiler.

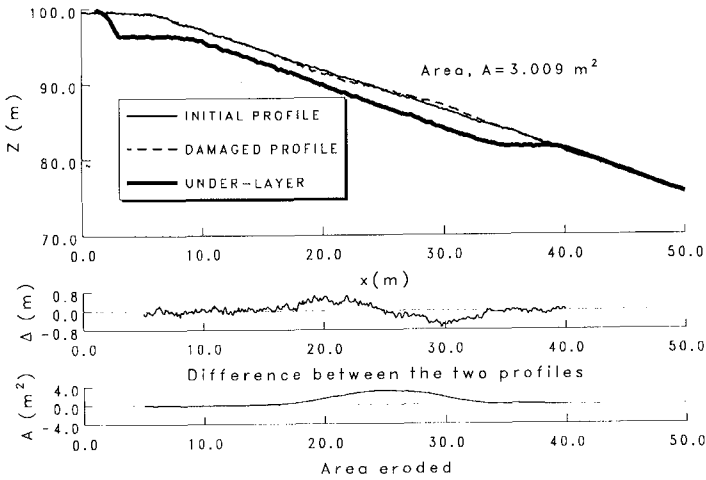


Figure 3 Typical average profile analysis.

where  $A_i(x)$  is the indefinite area integral and  $z_i$  and  $z_o$  are the damaged and original (undamaged) profile lines, respectively,  $x_o$  is the lower limit of integration (typically the top of the slope).  $S$  is determined as the maximum value of  $A_i(x)$  normalized by the square of the nominal diameter.

$$S_i = \frac{\max[A_i(x)]}{D_{n50}^2} \tag{6}$$

Figure 3 shows the results of average profile analysis - the upper plot shows the original and damaged profiles ( $z_o(x)$  and  $z_i(x)$ ), the middle plot shows the vertical difference between the two profiles,  $\Delta(x)$  and the bottom plot shows the indefinite integral,  $A_i(x)$ .

When sparse data is collected (e.g. foot method) curve fitting is often used to define a function describing the eroded area,  $A(x)$  (e.g. Medina et al, 1994 using a sinusoidal smoothing function). Previously integration had been performed only on the measured erosion by first removing the negative portion of the  $\Delta(x)$  curve in an attempt to increase the accuracy of the determination of  $S$  (e.g. Vidal et al, 1992). This method then requires accurate delineation of the range of integration since random noise in the  $\Delta(x)$  signal produces a positive bias in the integration. Recent refinements to NRC's profiling and data analysis methods have made such pre-processing of the data unnecessary.

While  $S$  analysis does give a reasonable measure of the average cross-sectional area of material eroded from the profile, it does not necessarily give sufficient information regarding the severity of damage. As illustrated in Figure 4 a value of  $S=3$  could represent a deep hole in the armour layer near the water line, or equally it could

represent shallow damage spread over a wider area. The significance of  $S$  depends strongly on stone size and armour layer thickness. When the damage index,  $S$  is applied to berm-type revetments the absolute value of  $S$  loses its physical significance although the stabilization of damage (attainment of an equilibrium profile) is characterized by a constant value of  $S$ .

### Analysis of Conventional Armour Layers

Van der Meer suggests using a value of  $S=2$  for the initiation of damage (zero-damage condition of Shore Protection Manual - 0 to 5% damage). Medina et al. suggest that lower values of  $S$  perhaps better describes the initiation of damage. Based on a series of 40 experiments on revetment stability performed at the National Research Council, it has been seen that  $S=2$  provides a good estimate of the start of damage. Lower damage levels have been seen to exhibit greater experimental variability.

Figure 5 illustrates a repeatability test, two realizations of the exact same test, this figure shows that agreement between the two experiments improves as  $S$  increases above 2. Figure 6 shows a comparison between the values of  $S$  obtained from profile analysis and the estimates of  $S$  based on visual stone counts. The good agreement obtained between these two methods illustrates the accuracy of the profiling method. Once the stone count gets above 60 to 80 stones the reliability of the visual method drops - it becomes difficult to visually monitor the movement of so many stones.

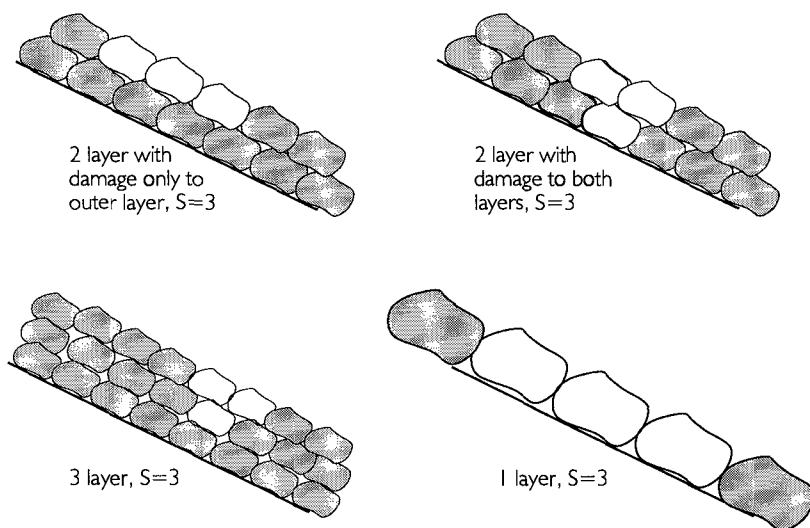


**Figure 4** Various possible damage configurations with same  $S$ .

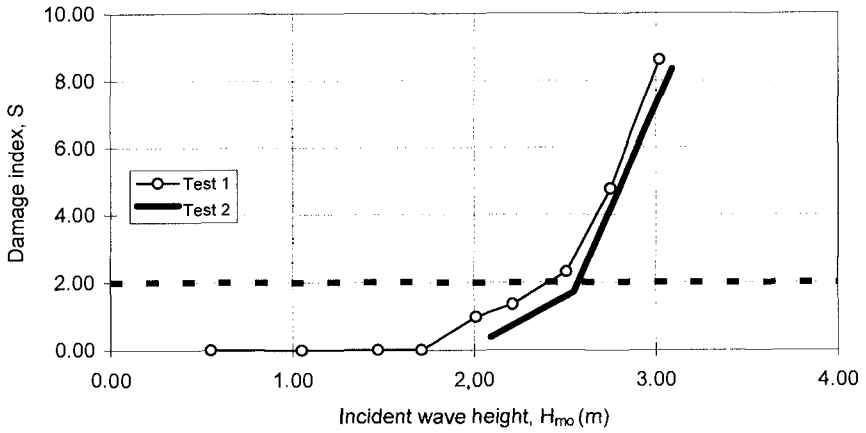


Figure 5 Repeatability test for typical revetment.

For berm breakwaters, the absolute value of  $S$  loses its direct relevance to damage (since many stones can move in the process of re-shaping to a stable profile). However, the shape of the damage evolution curves ( $S$  vs time,  $t$  or  $S$  vs number of waves,  $N$ ) does serve as a useful indication of performance. A stable berm should tend

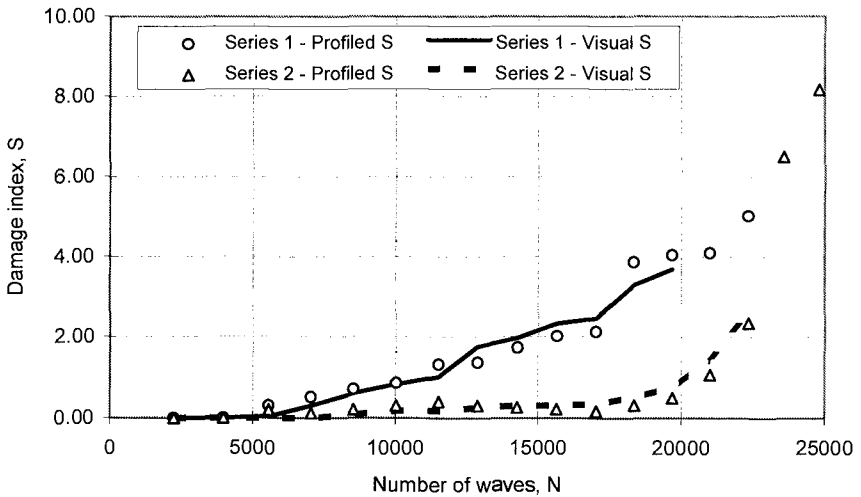
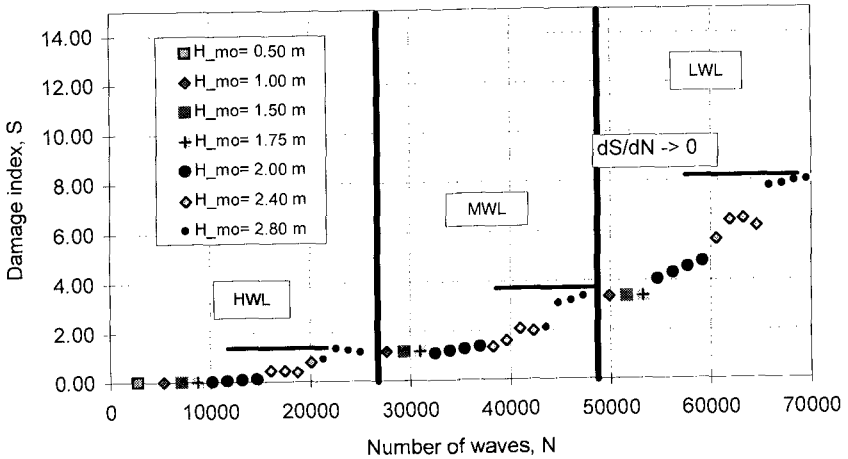


Figure 6 Comparison between  $S$  and  $S_{visual}$  for two typical revetment tests.



**Figure 7** S vs N for a berm tested and found stable ( $dS/dN=0$ ) at three water levels.

towards  $dS/dN=0$  under design conditions. This pattern is illustrated in Figure 7 where, during waves of  $H_{m0}=3.0$  m, the berm stabilizes and  $dS/dN$  approaches zero.

**Depth of cover**

The purpose of the outer revetment on a breakwater is to prevent the wave action from attacking the finer underlayers. Since failure of a breakwater is primarily caused by removal of the armour layer resulting in exposure and subsequent rapid removal of the finer underlayers it is reasonable to quantify the damage in terms of the existence of holes in the armour layer. For such analysis the quantity of material removed is inconsequential, it is the protection remaining which matters. This can be quantified as the depth of cover remaining on the structure,  $d_c$ . By measurement of the profile of the underlayer during construction and taking the difference between measured profiles of the revetment during testing and the reference underlayer profile one can calculate the thickness of the revetment, and the minimum thickness of the revetment,  $d_c$ . For most analyses the average minimum depth of cover is used. For example, in a series of two-dimensional flume experiments, nine profiles were taken over the 2 m width of the test section, the average profile was then subtracted from the average underlayer profile and the minimum cover thickness,  $d_c$  was computed. The resulting measured average minimum depth of cover can be compared to  $D_{n50}$ , such that when  $d_c$  drops below  $D_{n50}$  it can be inferred that there is some exposure of underlayer across the width of the test section. Should  $d_c$  drop to zero, the damage is severe enough that significant damage to the underlayer is likely to have occurred. Figure 8 shows typical depth of cover analysis for a revetment scheme. The left hand plot shows the profile (initial, damaged and under-layer), the armour layer thickness for both the initial and damaged conditions is shown in the right hand plot. The cover thickness is calculated as the slope-normal distance between the armour layer profile and the under-layer. The depth of cover,  $d_c$  is taken as the minimum of the cover thickness over the range of interest. As shown

in the plot,  $d_c$  for the initial conditions occurs at a different location than  $d_c$  for the damaged conditions.

When applied to berm-style revetments, the performance criteria is typically that the depth of cover,  $d_c$  should not drop below a certain level under design storm conditions. Figure 9 shows a  $d_c$  vs  $N$  plot for a berm-style structure (again tested at three water levels).

### Sliding failure

Other than the conventional unravelling of coastal structures due to the removal of individual stones by wave action, revetment failure can also occur by the large-scale sliding of the entire protection layer. This geotechnical failure mode has been discussed by other researchers but without an analytical framework within which to analyze such failures, the literature on this subject remains mostly anecdotal. In several of the revetment stability tests performed at NRC large-scale sliding of the armour layer was observed. Often this occurred with minimal prior damage to the structure. Several such failures were observed for steep sloped (1.6:1 and 1.7:1) structures. None were observed for structures with milder slopes (1.8:1 and 2.2:1). Figure 10 shows the measured profile of a revetment after sliding occurred near the mean water level (MWL). The profile of the slope after a sliding failure looks similar to other wave-eroded profiles - the key difference being the rapid rate of damage. This damage occurred during a single wave group (5 or 6 individual waves) and involved the downslope movement of the armour layer 'en masse'. Profile analysis is of little use in interpreting sliding - the main tools are visual observation and geotechnical analysis of the slope's factor of safety against sliding.

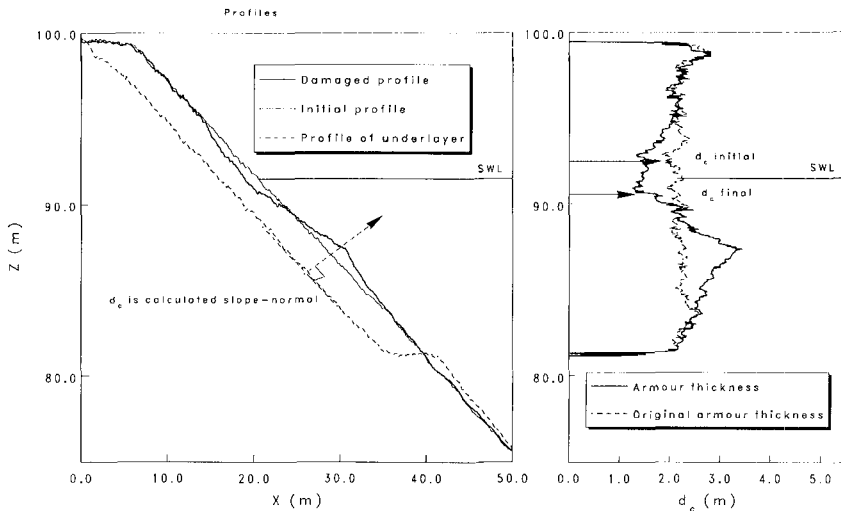
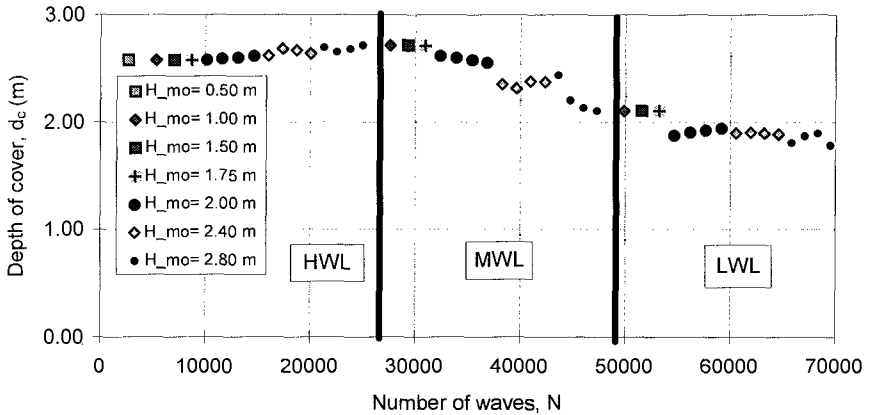


Figure 8 Typical depth of cover analysis.



**Figure 9** Depth of cover,  $d_c$  vs  $N$  for a berm.

A separate series of NRC experiments measuring the force exerted on breakwater revetments by wave action provides us with a reliable tool for estimating the wave loading on the revetment (Cornett and Mansard, 1994). These wave forces are then integrated into a limiting equilibrium translational sliding model. This uses conventional geotechnical stability analysis in conjunction with estimates of wave-induced lift and drag forces to evaluate the factor of safety of the slope against large-scale sliding failure. Comparisons between the sliding model results and breakwater testing have verified the ability of this method to predict the likelihood of sliding (Davies et al., 1994). This failure mode is most predominant for very steep breakwater slopes - 1:1.6 up to 1:1.3. Much of the literature on sliding of armour layers is related to the sliding which can occur once wave attack has created a hole in the armour layer, thereby providing an unsupported protection layer above the hole. This analysis is valid for such problems but is of more interest in the case of steep slopes where large-scale sliding is shown to occur without prior removal of the armour layer.

### Block model for sliding

Under the action of gravity alone, a slope of cohesionless soil will fail through translatory sliding. Under wave action, application of the driving force is limited to the zone around the still water line. In this case, the failure will be a block translational slide.

For the static problem, the planar translational slide predominates, and the factor of safety,  $FS$  (in the absence of external loadings) is simply the ratio of the tangent of the mobilised angle of shear resistance at failure,  $\phi'$  to the tangent of the slope angle,  $\theta$ .

$$FS = \frac{\tan \phi'}{\tan \theta} \tag{7}$$

The factor of safety is reduced when additional forces are exerted by wave action. The downslope shearing force due to wave action,  $F_{shear}$  can be estimated using the wave friction factor of Kamphuis (1975). The applicability of this type of analysis for the steep and very rough slopes of rubble-mound breakwaters has recently been verified at NRC by Cornett. In a series of hydraulic model tests, the wave forces exerted on breakwater armour have been measured and compared to the friction factor,  $f_w$  calculated using wave orbital velocity measurements just above the measuring section (see Cornett's figure 8 these proceedings, 1995). It is assumed that the wave-induced shear stress is applied uniformly over the region from the still water level down to  $H$  (measured vertically). This corresponds approximately to the range over which force measurements were made by Cornett.

Applying solitary wave theory to the breakwater slope, we can estimate the peak orbital velocity,  $u_b$  and the corresponding orbital amplitude,  $a_b$  as follows:

$$u_b = 0.61 \sqrt{gd_b} \quad \text{and} \quad a_b = \frac{u_b T}{2\pi} \tag{8}$$

here  $u_b$  is determined at an elevation equal to 1/2 the breaking depth of the wave (i.e. at  $z=d_b/2$ , where  $d_b=1.28 H$ ).

Applying the friction factor relationship of Kamphuis:

$$f_w = 0.4 \left( \frac{k_s}{a_b} \right)^{0.75} \quad \text{where} \quad k_s = 2D_{90} \tag{9}$$

This allows estimation of the shear stress acting on the surface,  $\tau$ :

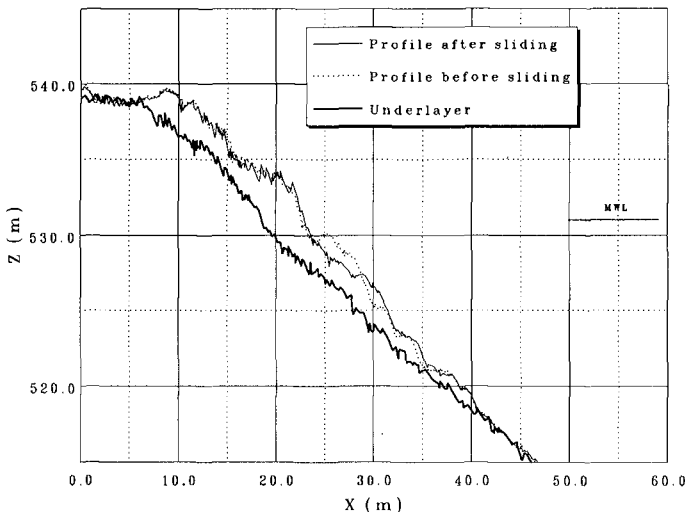


Figure 10 Profile after sliding near MWL.



$$\begin{aligned}
 \text{Weight: } W_1 &= 1/2 \text{ base} \times \text{height} \times \gamma' \\
 &= \gamma'/2 \ c\bar{d} \ (t_a + t_f/2) \\
 \text{Driving force along failure plane: } F_{D1} &= W_1 \sin \phi \\
 \text{Resisting force: } F_{R1} &= W_1 \cos \phi_1 \tan \phi'
 \end{aligned} \tag{12}$$

Forces acting on Block 2:

$$\begin{aligned}
 \text{Weight: } W_2 &= \frac{H \sin \theta}{2} \ (t_a + t_f/2) \ \gamma' \\
 \text{Driving force along failure plane: } F_{D2} &= W_2 \sin \theta + F_{\text{shear}} \\
 \text{where } F_{\text{shear}} &= \tau_{\text{waves}} \frac{H \sin \theta}{2} \\
 \text{Resisting force: } F_{R2} &= (W_2 \cos \theta - F_{\text{lift}}) \tan \phi'
 \end{aligned} \tag{13}$$

Forces acting on Block 3:

$$\begin{aligned}
 \text{Weight: } W_3 &= \gamma'/2 \ c\bar{d} \ (t_a + t_f/2) \\
 \text{Driving force along failure plane: } F_{D3} &= W_3 \sin \zeta \\
 \text{Resisting force: } F_{R3} &= W_3 \cos \zeta \tan \phi'
 \end{aligned} \tag{14}$$

The overall stability of the failure zone is calculated as the ratio of the sum of all resisting forces to the sum of all driving forces:

$$\begin{aligned}
 \text{Factor of safety, FS} &= \frac{\sum F_{\text{Resisting}}}{\sum F_{\text{Driving}}} \\
 \text{FS} &= \frac{F_{R1} + F_{R2} + F_{R3}}{F_{D1} + F_{D2} + F_{D3}}
 \end{aligned} \tag{15}$$

Using the above translational block sliding analysis, we can estimate the factor of safety of the revetment against failure.

Calculations have been made of the factor of safety against sliding for a slope of 1:1.7, an armour thickness of  $t_a=1.3\text{m}$ , a filter layer thickness of  $t_f=0.6\text{m}$  and a placement density of  $\gamma=1850\text{kg/m}^3$ . In this analysis, the shear strength of the rockfill is taken to be  $\phi'=42.8$ . This is based on the average of a series of tilting tests, where a cross-section of the dyke core, filter and armour layers were prepared in a rigid box, the box was then slowly lifted and the angle at which the slope failed was measured. This value corresponds well with reported natural angles of repose from field observations.

The translational block sliding analysis has been used to estimate the factor of safety against sliding for a given wave height for various layer geometries. In this analysis we have used  $H_{1/100}$  (roughly equal to  $1.8H_s$ ) as being representative of the larger waves in

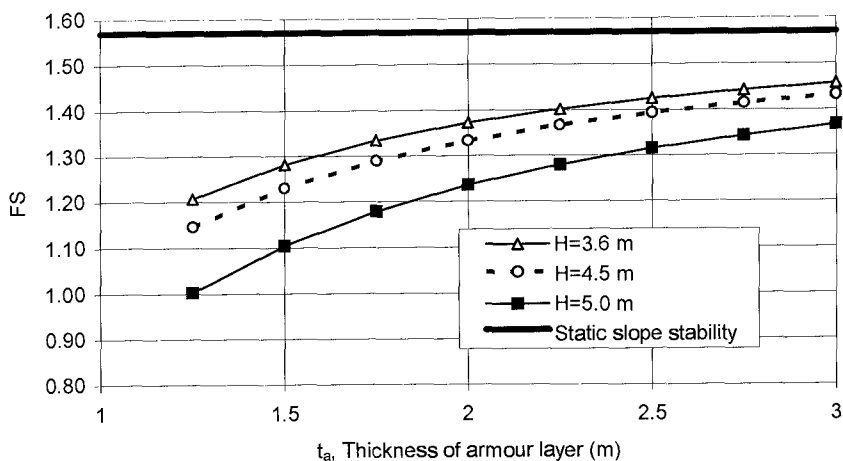


**Figure 12** Effect of armour layer thickness on factor of safety against sliding.

the time series. Figure 12 shows how the factor of safety varies with slope geometry. This analysis suggests that layer thickness has a strong influence on sliding stability (assuming that the preferred failure plane is through the filter layer).

This analysis suggests that single layer revetment is particularly prone to sliding failures and that the thickness of the armour layer is a significant factor in the sliding process. Thicker armour layers have a greater resistance to sliding failures which pass through the filter layer. Preliminary application of this translational block sliding analysis to observed sliding failures agrees well with observations, indicating that layer thickness and slope are the key factors affecting sliding potential. Detailed analysis of individual failures requires a less simplified model of the block sliding process. Recent work by Altae (1994) shows that a non-linear, stress and consolidation finite element model can be applied to this revetment stability problem. This work further supports the existence of a potential sliding failure zone in the filter layer just below the still water level. Work on these analysis methods is continuing.

## Conclusions

For profile analysis, reliable and efficient techniques have been developed using electro-mechanical profiling resulting in excellent agreement between  $S$  measured by profiling and  $S_{\text{visual}}$  measured from stone counting. There are inherent limitations in  $S$  as an analysis tool for breakwater damage due to the variability in the significance of  $S$  with structure type. Depth of cover,  $d_c$  has been shown to be a useful quantification of the damage related directly to the main failure criterion - the exposure of under-layers. This type of analysis is valid regardless of structure type.

Sliding has been seen to be a second failure mechanism for steep sloped structures. Visual observation, coupled with evaluation of the slope's factor of safety against sliding

in the presence of wave action is the best tool for damage analysis when sliding occurs. Block sliding analysis illustrates the importance of layer thickness in providing resistance to sliding. The translational block sliding model provides an analytic framework for interpreting the sliding potential of armour layers.

### Acknowledgements

The authors would like to thank Herman Claes, David Watson and Rod Girard without whose assistance and attention to detail this work would not have been possible. The input and advice of many of the staff of the Hydraulics and Geology and Soil Mechanics Departments of SEBJ are also gratefully acknowledged.

### References

- Altae, A. (1994). Feasibility study for numerical analysis of revetment stability under wave loading. Internal report by Anna Geodynamics Inc. to NRC (Ref. 93-1466/6297).
- Cornett, A.M. and Mansard, E.P.D. (1994) Wave stresses on rubble-mound armour. Proc. 24th Int. Coastal Engg. Conf. ASCE, New York, NY.
- Davies, M.H., Mansard, E.P.D. and Parkinson, F.E. (1994) Études sur modèles de la stabilité des ouvrages TA13 et KA3. NRC Controlled Technical Report IECE-CEP-CTR-001. Report prepared for Société d'énergie de la Baie James (in french).
- Hughes, S.A. (1993) Physical models and laboratory techniques in coastal engineering. Advanced Series on Ocean Engg. - Vol. 7. World Scientific Publishing, Singapore, 568 pp.
- Kamphuis, J.W. (1975) Friction factor under oscillatory waves. J. Waterways, Harbours and Coastal Engg. ASCE Vol. 101 (WW2). pp. 135-144.
- Latham, J.P., Poole, A.B., and Mannion, M.B. (1988) Developments in the analysis of armour layer profile data. Design of Breakwaters - Proc. of the Conference Breakwaters '88, ICE, Thomas Telford Ltd., London, UK, pp. 343-361.
- Medina, J.R., Hudspeth, R.T., and Fassardi, C. (1994) Breakwater armour damage due to wave groups. J. of Waterway, Port, Coastal and Ocean Engg., Vol. 120, No. 2, March/April 1994. pp. 179-198.
- Coastal Engineering Research Centre (1984) Shore Protection Manual. Coastal Engineering Research Center, U.S. Army Waterways Experiment Station, U.S. Govt. Printing Office, Washington, DC, 1984.
- van der Meer, J. (1988). Rock slopes and gravel beaches under wave attack. Ph.D. thesis, Delft Technical University, April. 152 pp.
- Vidal, C., Losada, M.A., Medina, R., Mansard, E.P.D. and Gomez-Pina, G. (1992). A universal analysis for the stability of both low-crested and submerged breakwaters. Proc. 23rd Int. Coastal Engg. Conf. ASCE, New York, NY.